RESEARCH PAPER

Structure-Based Virtual Screening of Natural Compounds Targeting CD45 for the Identification of Potential Anti-Psoriatic Agents

Komal D. Patil*, Dr. Minal R. Ghante
Department of Pharmaceutical Chemistry, Sinhgad Technical Education Society's,
Smt. Kashibai Navale College of Pharmacy (Kondhwa), Savitribai Phule Pune University, Pune 411048, India.
Corresponding author details:
Corresponding Author: Komal D. Patil*, Research Scholar
Mailing address: Sinhgad Technical Education Society's, Smt. Kashibai Navale College of Pharmacy (Kondhwa)
Tel.: +91 020 67571171
Mobile phone: +91-7045988540
E-mail: komaldpatil07@gmail.com
Corresponding author details:
Corresponding author: Dr. Minal R. Ghante, Principal
Mailing address: Sinhgad Technical Education Society's, Smt. Kashibai Navale College of Pharmacy (Kondhwa)
Affiliation:
Savitribai Phule Pune University, Pune, Maharashtra, India

Abstract
Background: Psoriasis is a chronic immune-mediated inflammatory disease involving various interactions between immune cells and keratinocytes. CD45 (protein tyrosine phosphatase receptor type C; PTPRC) is a leukocyte-specific receptor protein tyrosine phosphatase that regulates immune-cell signalling and represent a potential target for an inflammatory response. Natural products provide a structurally diverse source of bioactive compounds that may serve as potential leads for target-based drug discovery.
Objective: The present study aimed to identify and prioritize natural compounds with potential to interact with the catalytically active D1 phosphatase domain of CD45 using structure-based virtual screening, molecular docking, and in-silico ADMET and drug-likeness assessment.
Methods: The crystal structure of the human CD45 phosphatase domain (PDB ID: 1YGU) was used for structure-based screening. Nine selected natural compounds were docked into the experimentally characterized D1 binding pocket using AutoDock Vina, with TU-572 used as the reference compound. Predicted binding poses and protein–ligand interactions were analyzed & further evaluated for drug-likeness, pharmacokinetic characteristics, and potential toxicity using SwissADME and admetSAR.
Key docking findings: Dephostatin exhibited the most favourable predicted docking score (−7.6 kcal/mol), followed by Phosphatoquinones A (−7.3 kcal/mol), Purpurin (−6.8 kcal/mol), and Anonaine (−6.7 kcal/mol), compared with −6.5 kcal/mol for TU-572 which showed favourable interactions with key pocket residues.
ADMET findings: All screened compounds were predicted to comply with Lipinski's Rule of Five and showed high gastrointestinal absorption and excellent predicted $CaCO_2$ permeability. Dephostatin showed no predicted PAINS alert, whereas Phosphatoquinones A and Purpurin showed one and two PAINS alerts, respectively. Predicted skin permeation varied among the screened compounds.
Conclusion: The integrated docking and ADMET analysis identified Dephostatin, Phosphatoquinones A, and Purpurin as promising computational candidates for further investigation against CD45, with Dephostatin emerging as the leading candidate. These findings provide a preliminary structural basis for exploring natural products as potential CD45-targeting molecules in psoriasis. However, experimental CD45 phosphatase inhibition, selectivity, cellular, and pharmacological studies are required to validate the predicted activity and establish their potential as anti-psoriatic agents.
Keywords: CD45, psoriasis, natural compounds, virtual screening, molecular docking, ADMET.

How to cite this article: Komal D. Patil* Dr. Minal R. Ghante. Structure-Based Virtual Screening of Natural Compounds Targeting CD45 for the Identification of Potential Anti-Psoriatic Agents. Int J Drug Deliv Technol. 2026;16(78s):638-651. DOI: 10.25258/ijddt.16.78s.74.

Acknowledgement:
The authors sincerely acknowledge Savitribai Phule Pune University (SPPU), Pune, Maharashtra, India, for providing academic support and institutional affiliation for carrying out the present study.

1. Introduction:

The term "Psoriasis" refers to a chronic, immune-mediated inflammatory skin disease characterized

by persistent cutaneous inflammation, abnormal keratinocyte proliferation and differentiation, and dysregulated interactions between innate and adaptive immune cells. Although primarily recognized as a dermatological disorder, psoriasis is increasingly regarded as a systemic inflammatory condition associated with several comorbidities, including psoriatic arthritis, psychological disorders, cardiovascular disease, metabolic abnormalities, and hepatic complication [1-2]. The World Health Organization (WHO) has recognized psoriasis as a serious non-communicable disease and has highlighted the substantial physical, psychological, and social burden associated with the condition, including challenges related to diagnosis, access to appropriate treatment, and disease-associated stigma [3]. The global burden of psoriasis remains substantial. An analysis of Global Burden of Disease (GBD) data from 195 countries and territories covering the period from 1990 to 2017 demonstrated a persistent worldwide burden of psoriasis, with considerable variation in disease occurrence, clinical presentation, and associated comorbidities between populations and sexes [4]. Epidemiological studies have also identified important geographical and age-related variations in the distribution of psoriasis.

A study integrating GBD and PubMed/MEDLINE data reported that the estimated incidence of psoriasis increased from approximately 92 cases per 100,000 population in 1990 to 99 cases per 100,000 population in 2017. Higher incidence rates were reported in North America and Western Europe than in several Asian and Western Pacific populations, although differences in genetic background, environmental exposure, healthcare access, diagnostic practices, and disease ascertainment may contribute to these geographical variations [5]. The considerable global burden of psoriasis highlights the importance of understanding its underlying immunopathogenesis for the development of more effective and mechanism-based therapeutic strategies. Psoriasis results from a complex interaction among dendritic cells, T lymphocytes, keratinocytes, and other components of the innate and adaptive immune systems. Among the major inflammatory pathways implicated in psoriasis, the interleukin-23 (IL-23)/T helper 17 (Th17) axis has emerged as a central regulatory pathway. Following activation by environmental, genetic, or physiological stimuli, antigen-presenting cells, particularly dendritic cells, produce cytokines such as IL-23, which promote the expansion, maintenance, and pathogenic activity of Th17 cells. Activated Th17 cells subsequently produce inflammatory mediators, particularly IL-17A and IL-22, which act on keratinocytes and promote the expression of additional cytokines, chemokines, antimicrobial peptides, and other inflammatory mediators. This establishes a self-amplifying inflammatory circuit that contributes to epidermal hyperplasia, abnormal keratinocyte differentiation, leukocyte recruitment, and persistence of psoriatic lesions [6]. The immunopathogenesis of psoriasis therefore involves extensive crosstalk between innate and adaptive immune mechanisms rather than activation of a single inflammatory pathway. In genetically or immunologically susceptible individuals, environmental and physiological triggers—including psychological stress, infection, trauma, and other external stimuli—may contribute to initiation or exacerbation of disease. These stimuli can influence antigen-presenting cells, keratinocytes, and lymphocytes, thereby promoting the production of cytokines and chemokines that sustain cutaneous inflammation. Several cytokines and immune mediators have been implicated in this network, including IL-6, IL-21, IL-23, IL-17, IL-22, granulocyte-macrophage colony-stimulating factor (GM-CSF), interferon-γ (IFN-γ), tumor necrosis factor-α (TNF-α), IL-10, IL-25, IL-27, and other regulatory molecules [7,8]. However, their individual contributions differ according to the stage and cellular context of the disease, with the IL-23/IL-17 axis considered one of the most important pathogenic pathways in established psoriasis. **Figure 1** provides a schematic representation of the major immunological events involved in psoriasis, illustrating dendritic-cell activation, IL-23-mediated Th17 responses, cytokine-driven keratinocyte activation, innate–adaptive immune crosstalk, and the development and maintenance of chronic cutaneous inflammation [6]. Collectively, these mechanisms provide a rationale for targeting key regulatory proteins within immune-signalling pathways as potential strategies for the development of novel anti-psoriatic therapies. The interleukin-23 (IL-23)/T helper 17 (Th17) axis is considered a central pathway in the immunopathogenesis of psoriasis and contributes to the development of several associated comorbidities. In genetically susceptible individuals, various triggers, including psychological stress, physiological stress, infections, trauma, and environmental factors, can initiate or exacerbate immune dysregulation. These stimuli activate antigen-presenting cells, particularly dendritic cells, which produce IL-23 and promote the differentiation, expansion, and maintenance of pathogenic Th17 cells. Activated Th17 cells subsequently secrete pro-inflammatory cytokines, including IL-17, IL-22, tumour necrosis factor-α (TNF-α), interferon-γ (IFN-γ), granulocyte-macrophage colony-stimulating factor (GM-CSF), IL-21, and other inflammatory mediators, thereby amplifying keratinocyte activation and sustaining chronic inflammation. Additional cytokines, such as IL-6, IL-25, IL-27, IL-4, and the regulatory cytokine IL-10, further modulate immune responses and contribute to the complex cytokine network involved in psoriasis pathogenesis [7,8].

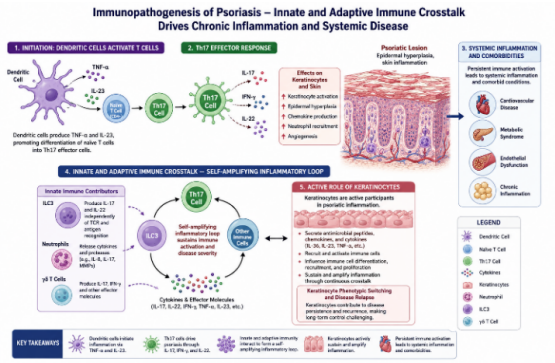

Figure No.1 Immunopathogenesis of psoriasis: interplay between innate and adaptive immune responses and the role of keratinocytes in chronic inflammation.

Understanding the contribution of inflammatory mediators to the onset and progression of psoriasis also provides a rationale for examining the mechanisms and limitations of currently available therapeutic approaches. Treatment selection is primarily guided by disease severity, extent of skin involvement, anatomical site, impact on quality of life, presence of psoriatic arthritis or other comorbidities, previous treatment response, and patient-specific factors. The therapeutic objectives include reduction of erythema, scaling, plaque formation, pruritus, and inflammation, as well as prevention of disease progression, relapse, and long-term complications. Current management strategies include topical therapies, phototherapy, conventional systemic agents, biologic therapies, and targeted small-molecule drugs.

Because psoriasis predominantly affects the skin, topical therapy is generally preferred as an initial treatment option for patients with localized or mild-to-moderate disease. Common topical treatments include corticosteroids, vitamin D analogues such as calcipotriol, corticosteroid–vitamin D analogue combinations, topical retinoids, calcineurin inhibitors, and keratolytic agents. Patients with extensive, moderate-to-severe, or treatment-resistant disease may require phototherapy or systemic treatment with agents such as methotrexate, cyclosporine, and acitretin. Although these treatments can provide substantial clinical benefit, their use may be limited by treatment-specific adverse effects and monitoring requirements. Prolonged or inappropriate use of topical corticosteroids may result in skin atrophy and other local or systemic adverse effects, whereas methotrexate, cyclosporine, and acitretin are associated with important safety concerns, including hepatotoxicity, nephrotoxicity, and teratogenicity, respectively. Phototherapy is effective for many patients but may involve repeated treatment sessions and cumulative exposure-related risks [9].

The introduction of biologic therapies targeting key inflammatory pathways, including tumour necrosis factor-α (TNF-α), interleukin-12/23 (IL-12/23), IL-17, IL-23, and IL-36, has significantly improved the therapeutic management of moderate-to-severe psoriasis. Many of these agents achieve substantial improvements in Psoriasis Area and Severity Index (PASI) responses, including PASI 75 and PASI 90. Nevertheless, important limitations remain, including increased susceptibility to certain infections, immunogenicity, paradoxical inflammatory reactions, primary or secondary loss of response, high treatment costs, and, for many biologic agents, the need for parenteral administration. In parallel, small-molecule therapies targeting Janus kinases (JAKs), tyrosine kinase 2 (TYK2), and phosphodiesterase-4 (PDE4) have expanded the therapeutic landscape. However, these agents also possess pathway-specific safety considerations and may not provide sustained or adequate responses in all patients [9]. Despite substantial advances in psoriasis treatment, a subset of patients continues to experience inadequate therapeutic response, intolerance, relapse, or loss of efficacy. These limitations emphasize the continuing need for the identification of novel therapeutic targets and agents that can provide effective, selective, durable, and potentially more accessible disease control. In this context, modulation of upstream regulators of immune-cell activation may represent a complementary strategy to direct cytokine blockade [9]. CD45, encoded by the protein tyrosine phosphatase receptor type C (PTPRC) gene, is a leukocyte-restricted receptor-type protein tyrosine phosphatase that plays an important role in regulating antigen receptor signalling. CD45 is abundantly expressed on T lymphocytes and modulates the phosphorylation status of Src-family kinases, particularly lymphocyte-specific protein tyrosine kinase (Lck) and Fyn, thereby influencing the threshold and magnitude of T-cell receptor (TCR) signalling. Through its intracellular protein tyrosine phosphatase domain, CD45 regulates tyrosine phosphorylation of signalling proteins and can exert either positive or negative effects on immune-cell signalling depending on the substrate, cellular context, and activation state [10,11]. The central involvement of dysregulated T-cell responses and inflammatory signalling in psoriasis provides a biological rationale for investigating regulatory molecules involved in T-cell activation. Persistent activation of pathogenic T-cell populations contributes to the production of inflammatory cytokines and maintenance of the chronic inflammatory environment characteristic of psoriasis. Given the established role of CD45 in regulating TCR-associated signalling, modulation of CD45 activity could potentially influence downstream T-cell responses and inflammatory mediator production. However, the direct contribution of CD45 to psoriasis pathogenesis and the therapeutic consequences of its pharmacological modulation remain insufficiently characterized.

Therefore, CD45 should be considered a potential upstream regulatory target worthy of investigation rather than an established therapeutic target for psoriasis [10-12]. Importantly, CD45 is essential for normal immune-cell development and signalling; consequently, complete or nonspecific inhibition could potentially interfere with physiological immune responses. A strategy based on selective modulation of CD45 phosphatase activity may therefore be more desirable than indiscriminate inhibition. Identification of structurally diverse compounds capable of interacting selectively with the CD45 catalytic domain could provide a foundation for investigating CD45 as a novel therapeutic target in psoriasis. This rationale supports the exploration of computational approaches for the identification and prioritization of potential CD45 modulators before experimental validation. Natural products represent a valuable source of structurally diverse bioactive molecules for early-stage drug discovery. Plants, microorganisms, marine organisms, and other natural sources produce chemically diverse secondary metabolites with a broad range of biological activities, including anti-inflammatory, immunomodulatory, antioxidant, and enzyme-inhibitory effects [13]. The structural diversity of natural products can provide useful chemical scaffolds for identifying molecules capable of interacting with therapeutically relevant protein targets. In the context of psoriasis, several natural products have demonstrated anti-inflammatory or immunomodulatory activities; however, compounds specifically reported to interact with or inhibit CD45 require careful evaluation of the available experimental evidence. **Table 1** summarizes the natural products selected in the present study based on their reported biological activity and/or potential relevance to CD45 inhibition [14].

Accordingly, the present study aimed to identify and prioritize potential natural-product-based CD45 inhibitors through a structure-based virtual screening approach followed by molecular docking analysis and evaluation of drug-likeness and pharmacokinetic/ADMET properties. This computational workflow was designed to identify promising CD45-interacting candidates that may serve as preliminary leads for the future development of novel anti-psoriatic agents.

2. Materials and Methods

2.1 Protein Preparation

The three-dimensional crystal structure of CD45 tyrosine phosphatase was obtained from the Protein Data Bank **(PDB ID: 1YGU)**. The structural information of the selected protein is presented in **Table 2**[15]. The protein structure was prepared for molecular docking using BIOVIA Discovery Studio 2024[16]. Based on the structural region represented in the selected PDB entry, the relevant amino acid residues (608–890) were retained for the docking study, while the remaining residues were excluded from the docking construct. Water molecules, heteroatoms, and the co-crystallized ligand were removed from the protein structure. Polar hydrogen atoms were subsequently added, and missing structural elements were corrected using BIOVIA Discovery Studio 2024. The prepared protein was subjected to energy minimization and structural optimization prior to docking. The resulting protein structure was then converted into the appropriate format using AutoDock Tools for molecular docking with AutoDock Vina [17].

TU-572, a previously reported potent CD45 inhibitor, was selected as the reference compound for evaluating the docking protocol and comparing the predicted binding interactions of the screened compounds[18]. The chemical structure of TU-572 is presented in **Figure 2**.

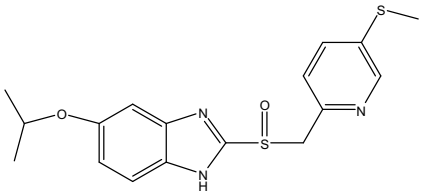

Figure 2: Structure of TU-572

2.2 Ligand Preparation, Molecular Docking, Validation, and ADMET Prediction

The selected natural compounds were sketched using ChemDraw software[19] and converted into three-dimensional structures. The resulting structures were subjected to geometry optimization and energy minimization using an appropriate molecular mechanic's force fields prior to molecular docking. The prepared compounds were subsequently docked against the catalytic domain of CD45 using AutoDock Vina to evaluate their predicted binding affinities and interactions within the active-site region. The docking grid was centered on the catalytic binding pocket using the coordinates **X = 15.232, Y = −10.938, and Z = 59.501**. A grid-box dimension of **40 × 40 × 40 Å** was used to provide sufficient coverage of the active-site cavity and surrounding residues. Docking simulations were performed under identical conditions for all selected compounds, and the resulting binding affinities were recorded in kcal/mol. The docked conformations were ranked according to their predicted binding affinity, and the binding modes of the top-ranked compounds were subsequently examined.

TU-572 was used as the reference CD45 inhibitor for comparative analysis [18]. The predicted binding orientation and molecular interactions of TU-572 were compared with previously reported structural interaction data. The docking poses of the screened compounds were analysed using BIOVIA Discovery Studio Visualizer, with particular attention to hydrogen bonding, hydrophobic interactions, π–π interactions, and electrostatic interactions with residues within the binding pocket.

Because the crystal structure used in the present study (PDB ID: 1YGU) contains a co-crystallized phosphotyrosine-containing peptide rather than the small-molecule reference inhibitor TU-572, conventional ligand redocking based on root-mean-square deviation (RMSD) could not be directly applied to TU-572. Therefore, the docking protocol was assessed through standardized preparation and docking conditions, comparison of the predicted binding mode of TU-572 with its reported interaction profile, and comparative analysis of the binding orientations and residue-level interactions observed for the screened natural compounds. The same docking parameters and binding-site coordinates were applied consistently across the reference and screened compounds.

2.3 ADMET and Drug-Likeness Prediction

The pharmacokinetic, drug-likeness, and toxicity profiles of the selected natural compounds were predicted using the SwissADME and admetSAR online platforms [20,21]. The evaluated parameters included Lipinski's Rule of Five, gastrointestinal absorption, blood–brain barrier permeability, CaCO permeability, PAINS, and skin permeation coefficient (Kp).

Table No .1: Natural CD45 tyrosine phosphatase inhibitors

Name of the molecule	Structure of the molecule	Source	IC_{50} (µM)	SMILES Notation	Molecular Weight	Chemical Formula
Dephostatin	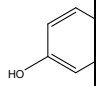	*Streptomyces* sp.	7.70	CN(C1=C(C=CC(=C1)O)O)N=O	168.1520	$C_7H_8N_2O_3$
Anonaine	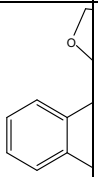	*Rollinia ulei*	17	[H][C@@]12CC3=CC=CC=C3C4=C1C(CCN2)=CC5=C4OCO5	265.3120	$C_{17}H_{15}NO_2$
Roemerin	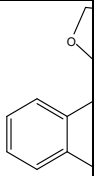		107	CN1CCC2=CC3=C(OCO3)C4=C2[C@@]1([H])CC5=CC=CC=C54	279.3390	$C_{18}H_{17}NO_2$
Nornuciferine	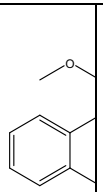		5.3	COC1=C(OC)C2=C3[C@@](NCCC3=C1)([H])CC4=CC=CC=C42	281.3550	$C_{18}H_{19}NO_2$
Phosphatoquinones A		*Streptomyces* sp.	28	C/C(C)=C\CC/C(C)=C/C[C@]12C(C3=C(C([C@]1(O2)C)=O)C(O)=CC(O)=C3)=O	356.4180	$C_{21}H_{24}O_5$
Phosphatoquinones B	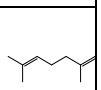		2.9	CC1=C(C/C=C(CC/C=C(C)\C)\C)C(C2=C(C(O)=CC(O)=C2)C1=O)=O	340.4190	$C_{21}H_{24}O_4$
Dihydrocaroli c acid	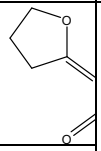	*Aspergillus niger*	6.7	C=C1C(/C(C(O1)=O)=C2CCCO/2)=O	180.1590	$C_9H_8O_4$
Penitricin D	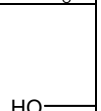		27.4	C=C1C(O)C1=O	84.0211	$C_4H_4O_2$
Purpurin	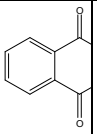	*Rubia cordifolia* L.	5.97	O=C(C1=C2C(O)=C(O)C=C1O)C3=CC=CC=C3C2=O	256.2130	$C_{14}H_8O_5$

Table No. 2: Protein Information

Sr. No.	Field	Value	Sr. No.	Field	Value
1	PDB ID	1YGU	10	Organism	Homo sapiens, Murine polyomavirus (strain A2)
2	Resolution	2.90 Å	11	Expression System	Escherichia coli BL21
3	Method of Characterization	X-Ray Diffraction	12	Co-crystallized ligand	Phosphotyrosine-containing peptide (pTyr peptide)

4	Mutation	Yes	13	Peptide source	Polyomavirus middle T antigen
5	R-value	0.305 (Depositor)	14	Peptide length	4 amino acids
6	R-value	0.262 (Depositor)	15	Modified residue	PTR (O-phosphotyrosine)
7	R-value Observed	0.262 (Depositor)	16	Active site co-ordinates	15.232, -10.938, 59.501
8	Enzymes Classification	Hydrolases	17	Size of the grid box	40 40 40 Å
9	Enzyme Commission Number	EC 3.1.3.48 (Protein-tyrosine-phosphatase)			

The predicted pharmacokinetic and toxicity profiles were used to prioritize compounds exhibiting favourable drug-likeness, potential oral bioavailability, and acceptable predicted safety characteristics for further consideration as potential CD45-targeting candidates.

3. Results

3.1 Structural Analysis of CD45 and Identification of the D1 Binding Pocket

The crystal structure of the intracellular phosphatase region of human CD45 was retrieved from the Protein Data Bank using PDB ID **1YGU**. The structure was determined by X-ray crystallography at a resolution of **2.90 Å** and contains two homologous protein tyrosine phosphatase domains, designated D1 and D2. The D1 domain represents the catalytically active phosphatase domain, whereas D2 is a catalytically impaired pseudo-phosphatase domain. The experimentally bound phosphotyrosine-containing peptide was located within the D1 active-site region, supporting the selection of D1 as the principal target domain for subsequent structure-based docking analysis.

Analysis of the D1 binding region using BIOVIA Discovery Studio identified several residues surrounding the experimentally bound phosphotyrosine-containing peptide, including Tyr658, Asp660, Arg704, Asp796, His797, Ser828, Ser829, Ala830, Gly831, Val832, Gly833, Arg834, Thr835, and Gln872. These residues define the structural environment of the D1 phosphatase binding pocket and were subsequently considered during analysis of the docked compounds. The two-dimensional representations of the CD45 structure and D1 binding pocket are presented in **Figure 3**.

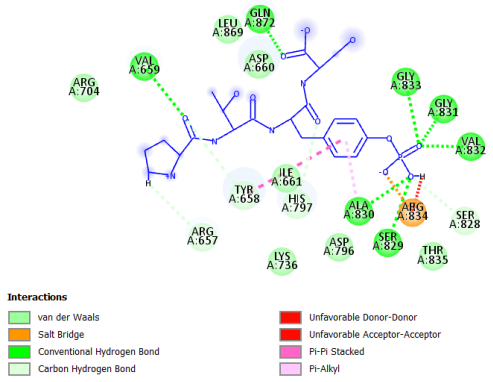

Figure 3. Two-dimensional structure and binding-site architecture of human CD45 (PDB ID: 1YGU)

3.2 Virtual Screening

A focused structure-based virtual screening approach was applied to evaluate **nine natural compounds** against the catalytically active D1 phosphatase domain of CD45. **TU-572** was included as the reference compound to provide a comparative benchmark for evaluating the predicted binding characteristics of the natural compounds. All compounds were subjected to the same docking protocol using the experimentally characterized D1 binding region.

The compounds exhibited variable predicted binding affinities and interaction profiles within the CD45 D1 pocket. Compounds with more favourable docking scores than the reference compound, together with interactions involving residues of the experimentally characterized binding region, were prioritized for further analysis.

3.3 Molecular docking

Molecular docking analysis was performed to investigate the binding behaviour of the selected compounds within the D1 phosphatase binding pocket of CD45. The docking poses were evaluated based on the predicted docking score, hydrogen-bond interactions, and interactions with key residues lining the binding pocket. The nine natural compounds were compared with the reference compound under the same docking conditions to identify compounds exhibiting favourable predicted binding characteristics. The docking results and major protein–ligand interactions are summarized in **Table No. 3**.

Molecular docking analysis revealed differences in the predicted binding behaviour of the reference compound and the nine natural compounds toward the CD45 D1 binding pocket. The reference compound TU-572 showed a docking score of −6.5 kcal/mol, forming conventional hydrogen bonds with Lys736 and His797, together with π-related interactions involving Tyr658, Ala830, and Asp796.

Among the natural compounds, Dephostatin exhibited the most favourable docking score (−7.6 kcal/mol), indicating the strongest predicted docking performance within the screened set. Dephostatin formed an extensive hydrogen-bonding network involving Gln872, Ala830, Gly831, Val832, Ser828, Gly833, Ser829, Asp796, and Tyr658. In addition, a π-anion interaction was observed with His797. The combination of a highly favourable docking score and multiple interactions within the D1 binding pocket suggests that Dephostatin may be a promising candidate for further investigation.

Phosphatoquinones A showed the second-most favourable docking score (−7.3 kcal/mol) and formed a conventional hydrogen bond with His797. It additionally showed π–π stacked interaction with Tyr658, π–π T-shaped interaction with Ala830, and π-alkyl interaction with Ile661. These interactions indicate favourable accommodation of the compound within the CD45 D1 pocket.

Purpurin, one of the natural compounds investigated, exhibited a docking score of −6.8 kcal/mol, which was more favourable than the reference compound TU-572 (−6.5 kcal/mol). Purpurin formed conventional hydrogen bonds with Arg734, Arg657, and Asn735, together with a π-cation interaction involving Arg704.

The favourable docking score combined with multiple polar and electrostatic interactions suggests

that Purpurin can be accommodated within the CD45 D1 binding pocket and warrants further investigation. Anonaine showed a docking score of −6.7 kcal/mol, slightly more favourable than the reference compound, with a conventional hydrogen bond involving Gln872 and a π-anion interaction with Glu874. Phosphatoquinones B and Roemerin showed a docking score of −6.5 kcal/mol, comparable to the reference compound. Roemerin formed a carbon–hydrogen bond with Gln633 and a π-anion interaction with Glu874, whereas Phosphatoquinones B formed a conventional hydrogen bond with Asn735 and π-related interactions with Arg734 and His797.

The remaining compounds showed comparatively less favourable docking scores. Nornuciferine exhibited a score of −6.1 kcal/mol and did not form a conventional hydrogen bond, although π-anion and π-alkyl interactions were observed with Glu874 and His797, respectively. Dihydrocarolic acid showed a score of −5.8 kcal/mol and formed several conventional hydrogen bonds involving Gly833, Arg834, and Ser829, but also exhibited an unfavourable interaction with Asp796. Penitricin D displayed the least favourable docking score (−5.0 kcal/mol), despite forming several conventional hydrogen bonds with His797, Ser828, Ala830, Gly831, Val832, and Arg834. The top-ranked compounds also formed favourable interactions with residues located within the CD45 D1 binding pocket, suggesting their potential to occupy and stabilize the target binding site.

3.4 ADMET and drug-likeness analysis

Following molecular docking, the selected compounds were subjected to in-silico ADMET profiling to assess their predicted pharmacokinetic characteristics and drug-likeness. The analysis included Lipinski's rule of five, gastrointestinal absorption, blood–brain barrier (BBB) permeability, $CaCO_2$ permeability, PAINS alerts, and skin permeation (Log Kp). These parameters were considered together with the docking results to provide a preliminary assessment of the overall suitability of the screened compounds as potential CD45-targeting candidates.

All ten compounds, including the reference compound TU-572, were predicted to satisfy Lipinski's rule of five, indicating that none of the screened molecules showed a violation of the selected physicochemical criteria. In addition, high gastrointestinal absorption was predicted for all compounds, suggesting favourable potential for gastrointestinal uptake if administered orally. The predicted $CaCO_2$ permeability was classified as excellent for all compounds, further supporting their predicted membrane permeability.

The predicted BBB permeability differentiated the compounds to some extent. TU-572, Dephostatin, Anonaine, Phosphatoquinones A, Phosphatoquinones B, Dihydrocarolic acid, Penitricin D, and Purpurin were predicted to be non-BBB permeable, whereas Roemerin and Nornuciferine were predicted to possess BBB permeability. For a peripherally acting target such as CD45, the absence of predicted BBB penetration may be considered favourable because unnecessary central nervous system exposure could potentially be avoided. However, this remains a computational prediction and requires experimental confirmation.

The PAINS analysis showed no alerts for TU-572, Dephostatin, Anonaine, Roemerin, Nornuciferine, and Penitricin D, whereas Phosphatoquinones A, Phosphatoquinones B, and Dihydrocarolic acid each showed one PAINS alert, and Purpurin showed two PAINS alerts. These alerts should be interpreted as potential assay-interference liabilities rather than direct evidence of toxicity or biological inactivity. Therefore, the PAINS alerts observed for Purpurin and the phosphatoquinones warrant additional consideration during subsequent experimental validation.

The predicted skin permeation values also varied among the compounds. Penitricin D showed the lowest Log Kp value (−6.98), followed by Dephostatin (−6.59), Dihydrocarolic acid (−6.58), and TU-572 (−6.52). In contrast, Phosphatoquinones B exhibited the highest Log Kp value (−4.50) among the screened compounds. Because Log Kp values describe the predicted tendency for skin permeation, these results may be relevant when considering potential topical delivery; however, they should not be interpreted alone as evidence of effective dermal penetration.

4. Discussion

Psoriasis is a chronic immune-mediated inflammatory disorder involving complex interactions between immune cells, inflammatory mediators, and keratinocytes. CD45 (PTPRC), a leukocyte-specific receptor-type protein tyrosine phosphatase, is an important regulator of immune-cell signalling. On this basis, modulation of CD45 represents a potentially relevant strategy for investigating upstream regulation of immune-associated signalling pathways. The present study therefore employed a structure-based computational approach to investigate natural compounds as potential CD45-targeting molecules.

The crystal structure of the tandem phosphatase domains of human CD45 (PDB ID: 1YGU) provided an experimentally characterized structural framework for the study. The presence of the catalytically active D1 domain and the experimentally bound phosphotyrosine-containing peptide enabled identification of the substrate-binding region used for docking. The residues identified around this region provide a structural basis for evaluating whether the screened compounds can occupy the D1 binding pocket and establish interactions with functionally relevant residues.

The docking analysis demonstrated considerable variation among the screened compounds. Dephostatin produced the most favourable predicted docking score (−7.6 kcal/mol), followed by Phosphatoquinones A (−7.3 kcal/mol), Purpurin (−6.8 kcal/mol), and Anonaine (−6.7 kcal/mol), whereas TU-572 produced a docking score of −6.5 kcal/mol. The more favourable predicted scores observed for several natural compounds suggest that these molecules may be capable of favourable accommodation within the selected CD45 D1 binding region. However, docking scores represent computational estimates of ligand–protein interactions and should not be interpreted as direct evidence of enzymatic inhibition or therapeutic efficacy.

Among the screened compounds, Dephostatin emerged as the strongest computational candidate. In addition to its favourable docking score, Dephostatin displayed an extensive network of interactions with residues distributed throughout the D1 binding region, including Gln872, Ala830, Gly831, Val832, Ser828, Gly833, Ser829, Asp796, and Tyr658. Such extensive contacts may contribute to stabilization of the predicted binding pose. The combined docking score and interaction profile therefore support the prioritization of Dephostatin for experimental evaluation. Nevertheless, the predicted interaction pattern does not establish whether Dephostatin inhibits CD45 enzymatic activity, and biochemical validation is required.

Phosphatoquinones A also demonstrated a favourable predicted binding profile, with a docking score of −7.3 kcal/mol and interactions involving His797, Tyr658, Ala830, and Ile661. The presence of hydrogen-bonding and π-related interactions suggests that the compound can be accommodated within the D1 binding region. However, its PAINS alert should be considered when interpreting its potential as a drug-discovery lead because nonspecific assay interference could complicate subsequent biological evaluation.

Purpurin is another notable candidate. Its docking score of −6.8 kcal/mol was more favourable than that of TU-572, and it formed several hydrogen-bond and π-cation interactions involving Arg734, Arg657, Asn735, and Arg704. These interactions indicate that the purpurin scaffold can establish multiple contacts within the CD45 D1 binding region. However, Purpurin generated two PAINS alerts, representing an important consideration for future experimental studies. Thus, its favourable docking result should be interpreted together with its potential assay-interference liability rather than considered solely on the basis of docking score. The ADMET analysis provided an additional basis for prioritizing the computational hits. All screened compounds were predicted to comply with Lipinski's Rule of Five, while high

Table No. 3. Docking Analysis

Type	Name of the Molecule	Docking Score /Binding Energy (Kcal /mol)	H-bonds	Key interactions	2D Interaction Diagram	3D Interaction Diagram
Reference	TU-572	-6.5	*LYS736, *HIS797	#TYR658, ##ALA830, ###ASP796	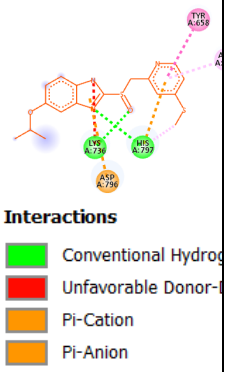	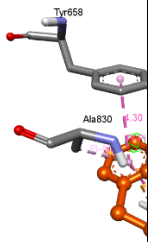
Natural	Dephostatin	-7.6	*GLN872, *ALA830, *GLY831, *VAL832, *SER828,	###HIS797	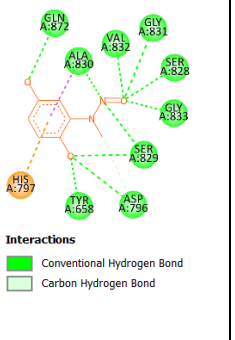	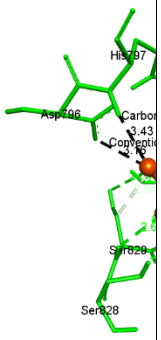
			*GLY833, *SER829, *ASP796, *TYR658			
	Anonaine	-6.7	*GLN872	###GLU874	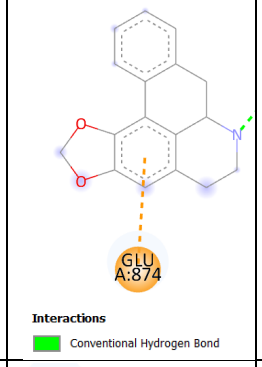	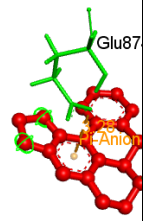
	Roemerin	-6.5	**GLN633	###GLU874	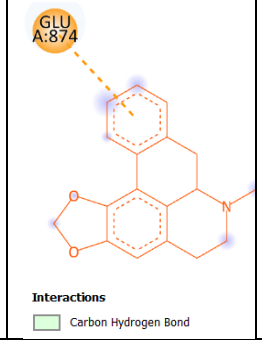	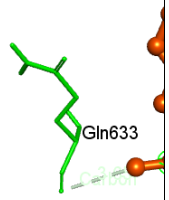

	Nornuciferine	-6.1	-	###GLU874, ####HIS797	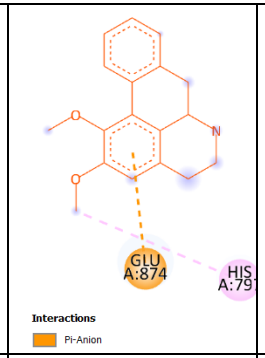	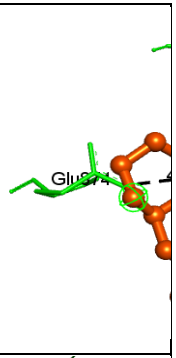
	Phosphatoquinones A	-7.3	*HIS797	#TYR658, ##ALA830, ####ILE661	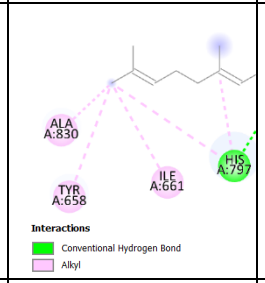	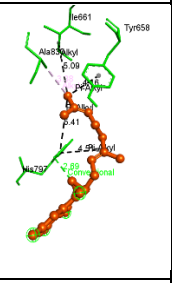
	Phosphatoquinones B	-6.5	*ASN735	###ARG734, ####HIS797	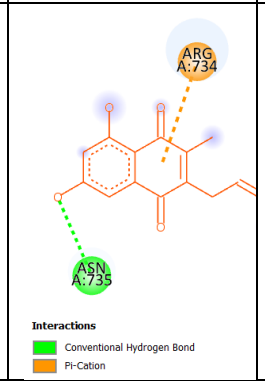	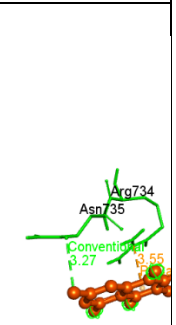
	Dihydrocarolic acid	-5.8	*GLY833, *ARG834, **SER829	***ASP796, ##HIS797, ####VAL832, #####TYR658, #####ALA830	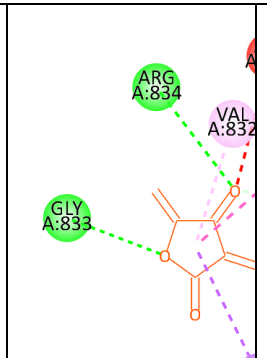	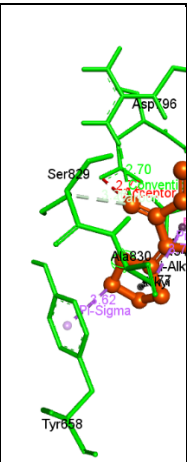
	Penitricin D	-5.0	*HIS797, *SER828, *ALA830, *GLY831, *VAL832, *ARG834	-	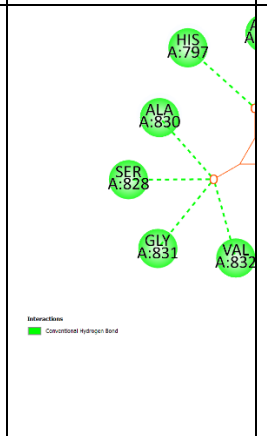	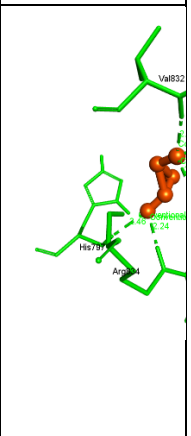

	Purpurin	-6.8	*ARG734, *ARG657, *ASN735	###ARG704	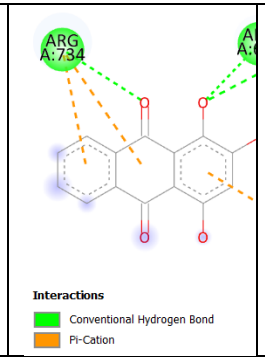	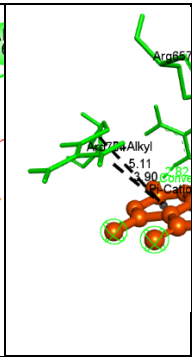

*Conventional Hydrogen Bond **Carbon Hydrogen Bond ***Unfavourable #Pi-Pi Stacked ## Pi-Pi T-shaped ### Pi Cation/Anion ####Pi-Alkyl #####Pi-Sigma

Table No. 4: ADMET Analysis

Name of the Molecule	Lipinski's Rule of Five	Gastrointestinal absorption	Blood-brain barrier permeability	CaCO permeability	PAINS	Log Kp (Skin permeation)
TU-572	Yes	High	No	Excellent	0	-6.52
Dephostatin	Yes	High	No	Excellent	0	-6.59
Anonaine	Yes	High	No	Excellent	0	-5.91
Roemerin	Yes	High	Yes	Excellent	0	-5.66
Nornuciferine	Yes	High	Yes	Excellent	0	-5.91
Phosphatoquinones A	Yes	High	No	Excellent	1	-5.16
Phosphatoquinones B	Yes	High	No	Excellent	1	-4.50
Dihydrocarolic acid	Yes	High	No	Excellent	1	-6.58
Penitricin D	Yes	High	No	Excellent	0	-6.98
Purpurin	Yes	High	No	Excellent	2	-5.14

gastrointestinal absorption and excellent predicted $CaCO_2$ permeability were observed for all compounds.

Most compounds were predicted not to cross the BBB, whereas Roemerin and Nornuciferine were predicted to possess BBB permeability. For a target primarily involved in immune-cell signalling, limited predicted CNS exposure could be considered advantageous; however, BBB predictions from computational platforms should not be interpreted as evidence of actual in-vivo distribution.

The predicted skin-permeation results are also relevant because psoriasis is primarily manifested in the skin and topical delivery may represent a potential route for anti-psoriatic therapy. However, the Log Kp values obtained from computational prediction should be interpreted cautiously. A favourable predicted skin-permeation value does not demonstrate adequate epidermal or dermal penetration, local bioavailability, or therapeutic efficacy. Experimental permeation studies would therefore be necessary before drawing conclusions regarding topical suitability.

When the docking and ADMET findings were considered collectively, Dephostatin emerged as the leading computational candidate, based on its most favourable predicted docking score, extensive interactions with the D1 binding pocket, predicted high gastrointestinal absorption, absence of predicted BBB penetration, compliance with Lipinski's criteria, and absence of PAINS alerts. Phosphatoquinones A showed strong predicted binding characteristics but requires additional consideration because of its PAINS alert. Purpurin also demonstrated favourable predicted binding relative to TU-572 but requires cautious interpretation because of its two PAINS alerts.

The findings therefore provide a preliminary computational basis for prioritizing Dephostatin, Phosphatoquinones A, and Purpurin for further investigation as potential CD45-targeting compounds. Importantly, the present findings should not be interpreted as evidence that these compounds are confirmed CD45 inhibitors or anti-psoriatic agents. Molecular docking predicts possible ligand–protein binding modes, whereas ADMET platforms provide computational estimates of pharmacokinetic and toxicity-related properties. Experimental CD45 phosphatase inhibition assays, cellular studies, selectivity assessment, and subsequent pharmacological evaluation are required to determine whether the computationally prioritized compounds possess genuine CD45 inhibitory activity and anti-psoriatic potential.

5. Conclusion

The present study employed a structure-based computational approach to identify potential natural compounds targeting the CD45 D1 phosphatase domain as prospective anti-psoriatic agents. The experimentally characterized CD45 structure (PDB ID: 1YGU) provided a rational structural basis for defining the D1 binding pocket, followed by focused molecular docking of nine natural compounds and one reference compound. The docking results demonstrated variable binding behaviour among the investigated molecules, with Dephostatin (−7.6 kcal/mol), Phosphatoquinones A (−7.3 kcal/mol), and Purpurin (−6.8 kcal/mol) showing favourable predicted binding compared with the reference compound TU-572 (−6.5 kcal/mol).

ADMET analysis further indicated generally favourable predicted drug-likeness among the screened compounds, with all molecules complying with Lipinski's rule of five and exhibiting high predicted gastrointestinal absorption and excellent $CaCO_2$ permeability. Among the screened molecules, Dephostatin emerged as the most promising overall candidate, based on its favourable docking score, extensive interactions within the CD45 D1 binding pocket, and favourable predicted ADMET profile without PAINS alerts. Phosphatoquinones A and Purpurin also demonstrated promising computational characteristics, although their predicted PAINS alerts warrant additional consideration.

Overall, the findings identify Dephostatin, Phosphatoquinones A, and Purpurin as potential CD45-targeting natural compounds and provide a computational basis for their further investigation in psoriasis-related drug discovery. Nevertheless, the present findings remain predictive, and in-vitro CD45 phosphatase inhibition assays, cellular studies, and subsequent pharmacological and toxicological evaluation are necessary to validate their biological activity and therapeutic potential.